Chapter 4
IRT Versus Moisture: In Situ Tests in Indoor Environment

4.1 Aim

The favourable results obtained when using IRT to assess moisture in full-scale models, under controlled conditions in the laboratory, promoted a new test campaign in order to evaluate the applicability of this technique to detect moisture now in walls of buildings in use. Also, the promising results of other authors when using IRT to assess moisture in situ (Avdelidis et al. 2003; Grinzato et al. 2010; Lerma et al. 2011; Edis et al. 2014, 2015; Menezes et al. 2015) encouraged this new stage. During this campaign, the passive approach was implemented and moisture was detected due to the effect of evaporative cooling.

Moisture in the walls under study had two different sources: rising damp and infiltration of rainwater. Rising damp was assessed in an exterior wall of a basement in a residential building, and infiltration of rainwater were evaluated in three locations, two exterior walls of a room in a residential building and in a wall of a classroom. The thermal images were compared with the results provided by a moisture detector.

4.2 Materials and Techniques

The devices used in this campaign were an infrared camera (Fig. 3.4a) and a moisture detector (Fig. 3.4b). The main specifications of the equipment are described in Sect. 3.2.2. Three different case studies were analysed, each with different sources (rising damp and infiltrations) causing the moisture problems:

- Exterior wall of a basement in a residential building (Fig. 4.1a), where the moisture source was rising damp;
- Exterior wall of a classroom in (Fig. 4.1b);
- Exterior walls of a room in a residential building (wall 1 in Fig. 4.1c and wall 2 in Fig. 4.1d), where infiltrations from rainwater occurred.

E. Barreira and R. M. S. F Almeida, *Infrared Thermography for Building Moisture Inspection*, SpringerBriefs in Applied Sciences and Technology,
https://doi.org/10.1007/978-3-319-75386-7_4

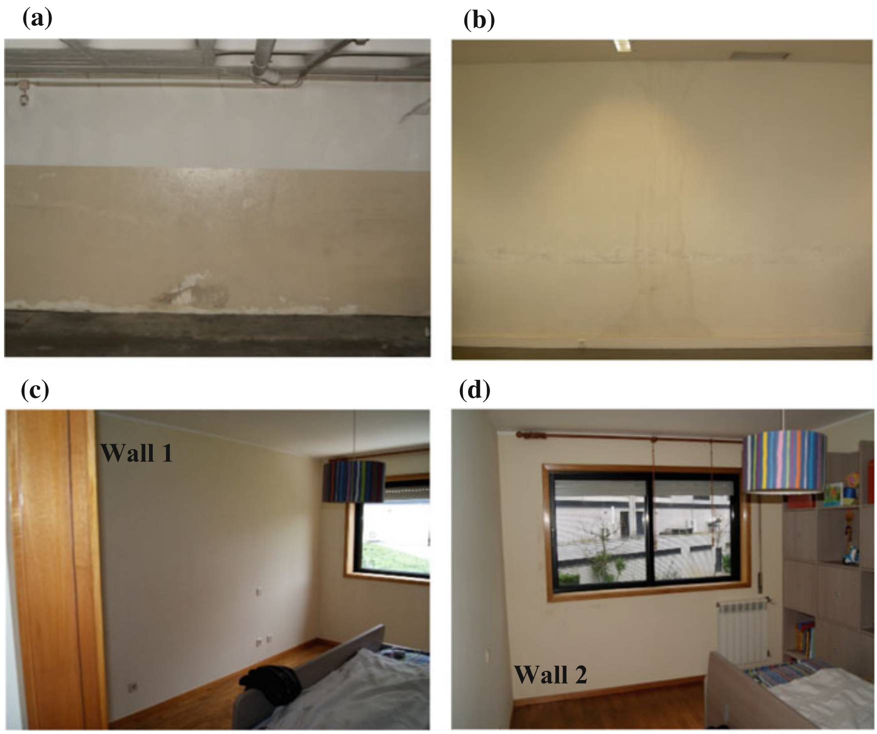

Fig. 4.1 Elements under study: **a** exterior wall of a basement in a residential building; **b** wall 1 of a room in a residential building; **c** wall 2 of a room in a residential building; **d** wall of a classroom in University of Porto

In this work, the IRT passive approach was used and the moist areas in the building components were assessed considering the effect of evaporative cooling. Thermal images were taken assuming an emissivity of 0.9 in the three set-ups because all walls were covered with cement plaster painted with light colour. The measurements were carried out after a rainy week.

To compare the results obtained by IRT with the ones provided by the moisture detector, the correlation between the relative scale of the detector results and the thermal images presented in Sect. 3.2.1 was used. Table 4.1 presents the characteristics of the grid used in each set-up. The spacing between dots depended on the area with visible degradation and the total area of the element (Barreira et al. 2016).

Table 4.1 Spacing between dots in the grids (in meters) for the assessment with the moisture detector

	Classroom	Room		Basement
		Wall 1	Wall 2	
Horizontal	0.30	0.30	0.30	0.20
Vertical				
Sound area	0.30	0.30	0.30	0.40
Damaged area	0.30	0.30	0.30	0.30

4.3 Results

4.3.1 Exterior Wall of a Basement in a Residential Building

The wall under study showed signs of degradation of the inner coating near the ground caused by rising damp (Fig. 4.1a). In the thermal image (Fig. 4.2a), a colder area near the ground, resulting from the evaporation of rising damp, is clearly displayed. The upper level of the colder area is above the visible degradation of the surface.

The results of the moisture detector (Fig. 4.2b) show that the moisture level in the wall was around 1.7 m from the ground, corresponding to a change in the superficial coating. The lower coating is less vapour permeable than the upper one, which can reduce superficial evaporation, increasing the amount of moisture in inner layers of the wall. When comparing the thermal image with the results of the moisture detector, they are not completely in accordance. One possible explanation may be related to the fact that IRT only detects surface evaporation, while the moisture detector assesses inner moisture.

The temperature profiles at 0.2 m from the ground (line A in Fig. 4.2a), at 0.7 m from the ground (line B in Fig. 4.2a) and at 1.2 m from the ground (line C in Fig. 4.2a), are displayed in Fig. 4.3. As expected, Line A, the nearest to the ground, presents the lower temperatures, followed by lines B and C. The temperature profile in line

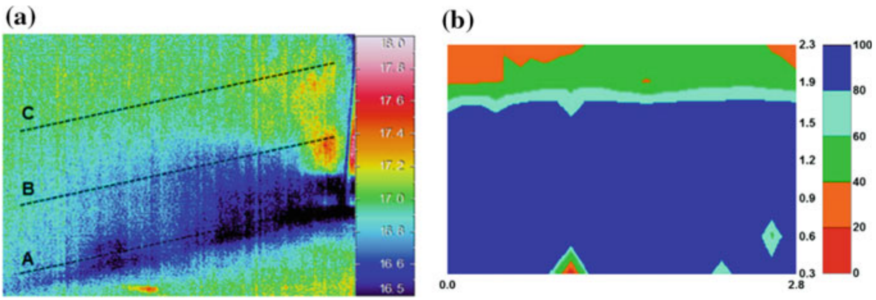

Fig. 4.2 Exterior wall of a basement in a residential building: **a** thermal image; **b** results of the moisture detector

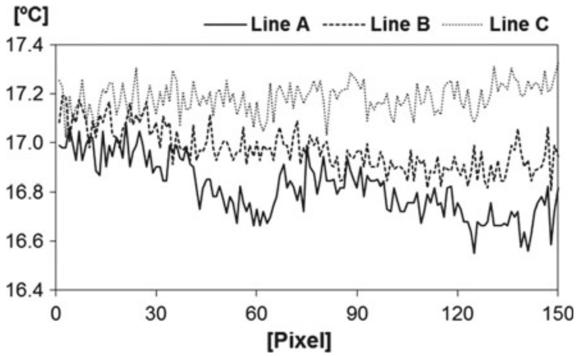

Fig. 4.3 Temperature profiles of an exterior wall of a basement in a residential building at 0.2 m from the ground through (line A), at 0.7 m from the ground (line B) and at 1.2 m from the ground (line C)

C indicates that the wall, at this level, was drier, because no relevant variations of the values between pixel 0 and 150 can be observed. In lines A and B, temperatures near pixel 150 are lower than the ones around pixel 0, which indicates higher moister problems near the corner.

Two critical zones can be pointed in line A, corresponding to the coating with greater degradation (between pixels 40 and 70 and between pixels 120 and 150, where temperatures are, on average, 16.8 and 16.7 °C, respectively). Due to the coating degradation, evaporation is more intense in these two zones and, thus, temperatures are lower.

The box plot representation of the temperature profiles at different levels (Fig. 4.4) points to higher variability of the values at line A and lower at line C. This result is due to a more intense evaporation at the bottom, where the highest amount of water is available, and also to the degradation of some areas of the coating that enhances the phenomenon. Smaller fluctuations in temperature at the highest level indicate that the amount of water reaching it is lower and temperature variations due to evaporation are not so evident.

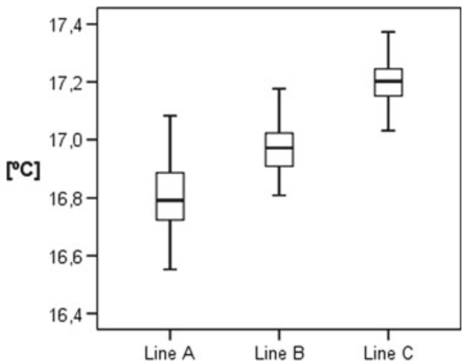

Fig. 4.4 Box plot representation of the temperature profiles of an exterior wall of a basement in a residential building at 0.2 m from the ground through (line A), at 0.7 m from the ground (line B) and at 1.2 m from the ground (line C)

4.3.2 *Exterior Walls of a Room in a Residential Building*

During the measurements, next to the corner and near the window, the coating of the two walls had visible signs of degradation caused by rainwater infiltration. The two walls were assessed individually (Fig. 4.1c, d). This infiltration had been detected before the test was performed and was not repaired by that time. Figure 4.5 shows the thermal images of the walls. The thermal images result from the assembly of individual images taken to restrict areas of each wall. Figure 4.6 shows the results obtained when using the moisture detector. Grey areas in Fig. 4.6a represent the position of the window and the radiator located in wall 1.

The thermal image of wall 1 displays lower surface temperatures around the left corner, under the window and at the top (Fig. 4.5a). The results of the moisture detector (Fig. 4.6a) showed that the wall is dry at the top, which indicates that the lower temperatures (dark blue) found in the thermal image correspond to a thermal bridge due to a beam. Although lower values have been measured with the moisture detector on the left vertical corner of the wall, at the thermal image, the lowest temperatures on this area (dark blue) are also related to a thermal bridge (structural column) and not only due to moisture. These considerations are supported by the information given by the structural plans of the building.

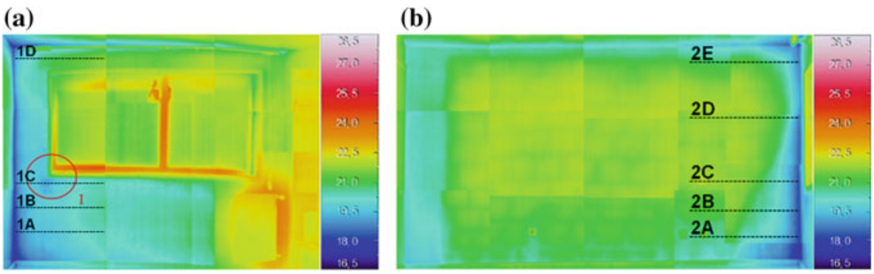

Fig. 4.5 Thermal images of the walls in a room: **a** wall 1; **b** wall 2

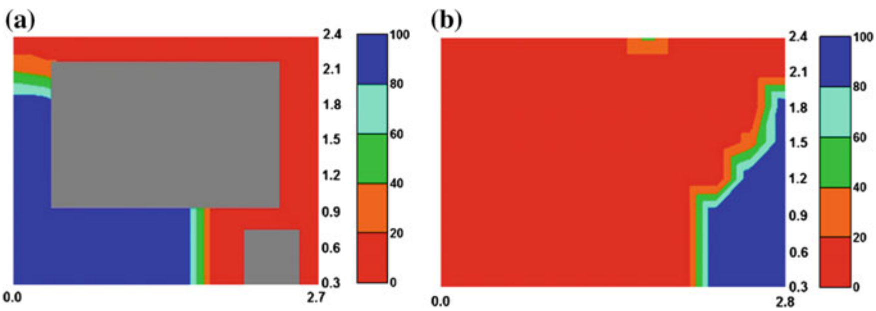

Fig. 4.6 Results of the moisture detector of the walls in a room: **a** wall 1; **b** wall 2

However, the surface temperature corresponding to the light blue colour results from the existence of moisture coming from outside. This conclusion was supported by the results of the moisture detector and by the existence of a damaged zone marked as I in Fig. 4.5a. Also, the visual inspection carried out on the exterior side of the wall revealed the existence of a crack. It must be stated that only the marked area is damaged in the inside. However, it is possible to assume that a larger area is affected by moisture, although not visually detected, taking into account the thermal image and the results of the moisture detector.

Figure 4.5b shows the thermal image of wall 2. Lower temperatures occur near the corners and at the top of the wall. The structural plans of the buildings indicate the presence of a beam and columns in those areas, which points to the existence of thermal bridges. However, there are clear differences between the colder areas on the left and right corners, indicating the presence of moisture in the right. The results of the moisture detector (Fig. 4.6b) support this conclusion, as the moister area is located near the right corner. Also, the existence of a crack on the exterior side of the wall in this area, as previously referred, strengthens this conclusion.

The temperature profiles of wall 1 at 0.3 m from the ground (line 1A in Fig. 4.5a), at 0.6 m from the ground (line 1B in Fig. 4.5a), at 0.9 m from the ground (line 1C in Fig. 4.5a) and at 2.4 m from the ground (line 1D in Fig. 4.5a) are displayed in Fig. 4.7. Figure 4.8 presents the temperature profiles for wall 2 (line 2A at 0.3 m, line 2B at 0.6 m, line 2C at 0.9 m, line 2D at 1.8 m and line 2E at 2.4 m in Fig. 4.5b).

Temperatures on lines 1A and 1B are very similar, although in line 1A the values are always lower. That may be related to the existence of a thermal bridge due to a beam. Although line 1C also presents temperatures similar to the ones of lines 1A and 1B, there are some critical areas between pixels 80 and 120 (point I in Fig. 4.5a) and between pixels 170 and 230, which are related to infiltrations of rainwater, as supported by the results of the moisture detector. Temperatures on line 1D are always higher as no moisture was detected at this level (Fig. 4.6a).

The temperature profiles of wall 2 (Fig. 4.8) show that at all levels there is an increase of surface temperature between pixels 0 and 10 related to a thermal bridge due to the existence of a column. However, at the lowest levels (lines 2A, 2B and

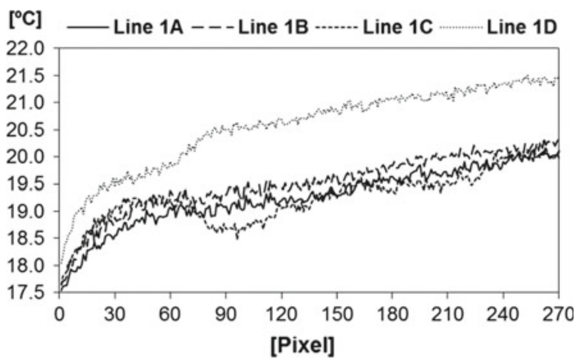

Fig. 4.7 Temperature profiles of wall 1 at 0.3 m from the ground through (line 1A), at 0.6 m from the ground (line 1B), at 0.9 m from the ground (line 1C) and at 2.4 m from the ground (line 1D)

Fig. 4.8 Temperature profiles of wall 2 at 0.3 m from the ground through (line 2A), at 0.6 m from the ground (line 2B), at 0.9 m from the ground (line 2C), at 1.8 m from the ground (line 2D) and at 2.4 m from the ground (line 2E)

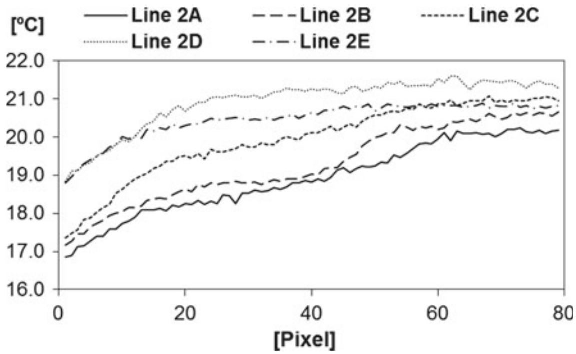

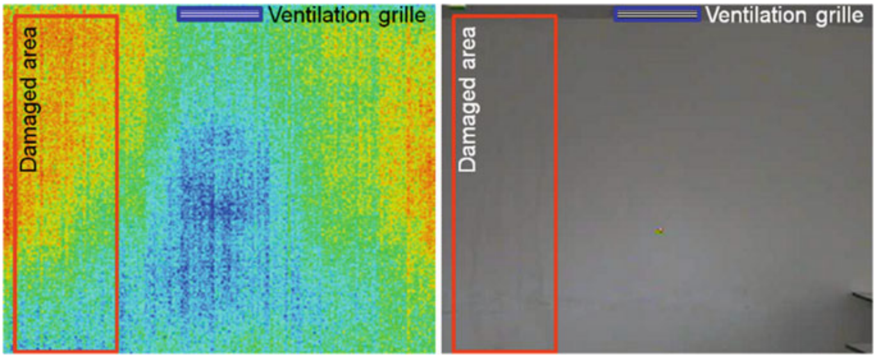

Fig. 4.9 Visible and thermal image of the wall under study in the classroom

2C), the superficial temperatures are lower, which indicates the existence of moisture that drops the values as a result of evaporation at the surface. Also, it is possible to detect that the moist area is larger at the bottom of the wall (line 2A) and decreases when the level is higher. In fact, the effect of moisture is noted until around pixel 60 at line 2A, around pixel 45 at line 2B and around pixel 20 at line 2C. Temperatures at lines 2D and 2E are very similar until around pixel 15, diverging from that point. The values are lower at line 2E due to the presence of a beam that decreases surface temperatures (thermal bridge).

4.3.3 Exterior Wall of a Classroom

By the time the measurements were carried out, the coating of the wall was damaged due to an infiltration of rainwater through the roof. This problem had already been detected and repaired two months before the test was performed. Figure 4.9 shows, respectively, the visible and the thermal image, and Fig. 4.10 shows the results of the moisture detector.

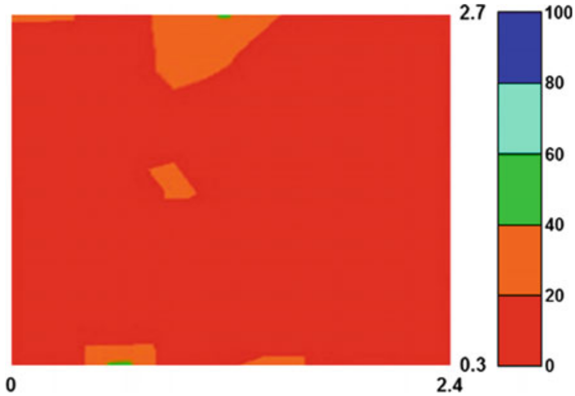

Fig. 4.10 Moisture detector results of the wall in the classroom

If not analysed carefully, the thermal image could lead to a misinterpretation of the results. In fact, the colder area (dark blue in Fig. 4.9) is not located where the coating is damaged but aligned with the ventilation grille located in the ceiling. The results of the moisture detector confirmed that there is no moisture in the wall, what was expected as the problem had already been repaired.

4.4 Discussion of the Results

Experimental tests showed that IRT is a valid diagnostic tool to evaluate moisture in building elements, when the source of humidity is rising damp and infiltrations of rainwater. However, in order to achieve reliable results, in some situations, it must be combined with other devices, namely a moisture detector to avoid misinterpretations.

Although moisture can be detected using the qualitative approach, the quantitative one proved to be very efficient, allowing extracting additional information. In fact, using the quantitative analyses of the thermal images, it was possible to identify critical areas that were not detected visually. These areas were highlighted by not only a sharp drop of surface temperature but also a larger variability of the values.

The use of complementary devices and/or information to support the findings of IRT proved to be of relevance. In two of the three case studies presented, misinterpretation of the results could have been a problem if a moisture detector was not used and if the structural plans of the building had not been analysed.

References

Avdelidis N, Moropoulou A, Theoulakis P (2003) Detection of water deposits and movement in porous materials by infrared imaging. Infrared Phys Technol 44(3):183–190

Barreira E, Almeida RMSF, Delgado JMPQ (2016) Infrared thermography for assessing moisture related phenomena in building components. Constr Build Mater 110:251–269

Edis E, Flores-Colen I, Brito J (2014) Passive thermographic detection of moisture problems in façades with adhered ceramic cladding. Constr Build Mater 51:187–197

Edis E, Flores-Colen I, Brito J (2015) Quasi-quantitative infrared thermographic detection of moisture variation in facades with adhered ceramic cladding using principal component analysis. Build Environ 94:97–108

Grinzato E, Cadelano G, Bison P (2010) Moisture map by IR thermography. J Mod Opt 57(18):1770–1778

Lerma JL, Cabrelles M, Portalés C (2011) Multitemporal thermal analysis to detect moisture on a building façade. Constr Build Mater 25(5):2190–2197

Menezes A, Gomes MG, Flores-Colen I (2015) In-situ assessment of physical performance and degradation analysis of rendering walls. Constr Build Mater 75:283–292